LWT - Food Science and Technology 65 (2016) 304–310

Contents lists available at ScienceDirect

LWT - Food Science and Technology

journal homepage: www.elsevier.com/locate/lwt

# Determination and modeling of contact angle of Canola oil and olive oil on a PTFE surface at elevated temperatures using air or steam as surrounding media

Alev Y. Aydar [a, c], Veronica Rodriguez-Martinez [b], Brian E. Farkas [a, b, *]

[a] Department of Food, Bioprocessing and Nutrition Sciences, North Carolina State University, Raleigh, NC 27695, USA
[b] Department of Food Science, College of Agriculture, Purdue University, West Lafayette, IN 47907, USA
[c] Department of Food Engineering, Faculty of Engineering, Celal Bayar University, Muradiye, Manisa 45140, Turkey

ARTICLE INFO

*Article history:*
Received 24 March 2015
Received in revised form
23 July 2015
Accepted 7 August 2015
Available online 10 August 2015

*Keywords:*
Contact angle
Interfacial tension
Vegetable oil
Steam
High temperature

ABSTRACT

Contact angles (CAs) of unused Canola and olive oils on polytetrafluoroethylene (PTFE) were measured, and the effect of oil type, surrounding media, and temperature evaluated. CAs were compared to values predicted by Girifalco-Good-Fowkes-Young (GGFY) equation, and GGFY combined with the Eötvös equation (GGFY-E). Finally, a relationship between the CA and interfacial tension for each oil type was obtained. CAs were measured by the sessile drop method (ramé-hart instrument co.). For oil-air systems, measurements were performed at 23 ± 1 °C, 40 °C, and then every 20 °C until reaching the oils' smoke point (olive oil: 180 °C, Canola oil: 200 °C). The same procedure was followed for oil-steam systems with first and second temperatures of 110 and 120 °C, respectively. Temperature and oil type had a significant effect ($P < 0.05$) on CAs, while no significant effect of surrounding media was observed. CAs decreased linearly as temperature increased (approximately 0.2°/°C). Error (E%) values were less than 10% for the majority of Canola oil systems and olive oil-air predicted CAs. Using Zisman plots, PTFE's surface tension estimates were determined using Canola and olive oil air systems (16.0 and 18.2 mN/m respectively); both systems showed a linear correlation ($r^2 = 0.99$) between interfacial tension and CA.



## 1. Introduction

According to the US Department of Agriculture (2014), world vegetable oil consumption has increased from 145.05 to 172.06 million tonnes during the last five years. An estimated of 73.4% of the total vegetable oil production is used for food purposes (USDA-FAS, 2014), and from this amount (approx. 126.3 million tonnes), 20% is destined to shallow and deep frying (Gunstone, 2002). Deep-fat frying is one of the oldest and most commonly used unit operations in food processing in homes and industry. Frying is a relatively low cost process, and the combination of temperature and oil uptake positively impact organoleptic attributes (e.g. flavor, texture, mouth-feel, and appearance) and the quality of the final product (Bouchon & Pyle, 2004; Saguy & Dana, 2003). Frying oil selection is based upon its oxidative stability, smoke point, foaming capabilities, melting point, flavor and nutritional value; examples of vegetable oils used for deep-fat frying include: Canola, corn, cottonseed, olive, palm, peanut, soybean, safflower, and sunflower (Erickson, 2007; Kochhar, 2001).

Frying is a complex process characterized by simultaneous heat and mass transfer, in which the food dehydrates and oil is absorbed into it. Oil uptake is an important quality factor of fried food; however, how the absorption phenomenon occurs is not completely understood (Bouchon, 2009). Several factors have been reported to affect oil uptake during frying including: pre- and post-frying treatments, temperature and time of frying, initial and final moisture content, crust structure (pore formation and size distribution), product geometry (surface area and roughness), oil quality (composition) and interfacial tension (Blumenthal, 1991; Bouchon, 2009; Bouchon & Pyle, 2004; Moreira, Sun, & Chen, 1997). The primary approaches to describe the mechanism of oil uptake consider the relationship between the uptake and moisture loss, capillary pressure, steam condensation, adhesion and drainage (Ziaiifar, Achir, Courtois, Trezzani, & Trystram, 2008). The effect of moisture loss occurs during frying when water from the food forms

* Corresponding author. 745 Agriculture Mall Drive, West Lafayette, IN 47907, USA.
*E-mail address:* bfarkas@purdue.edu (B.E. Farkas).

http://dx.doi.org/10.1016/j.lwt.2015.08.022
0023-6438/

steam. Depending on the resistance of the food's structure, steam can escape through weaker cellular structure, or remain trapped within the food matrix. In both cases, this allows oil uptake either by creating capillary pathways and pores, or by a vacuum effect due to post-frying steam condensation (Dana & Saguy, 2006; Ziaiifar et al., 2008). However, the vigorous escape of steam also limits oil uptake during frying, as it creates a barrier between the food and the oil (Bouchon, 2009).

It has been established that the main oil uptake occurs once the food is removed from the fryer and the food's temperature cools down (Moreira et al., 1997). In some areas of the fried food, the steam trapped inside the pores condensates and the internal pressure decreases while oil from the surface of the food enters the pores by suction (Mellema, 2003; Ziaiifar et al., 2008); whereas in other areas, oil is pulled into the pores and microchannels due to capillary forces (Dana & Saguy, 2006; Ziaiifar et al., 2008). After frying and as consequence of degradation, the layer of oil covering the food has a higher viscosity and contains more surfactant agents than the fryer oil poured into the fryer (Dana & Saguy, 2006; Rossi, Alamprese, Ratti, & Riva, 2009). Those changes in oil chemistry, in addition to the lower external temperature, increase the oil's wettability and adhesion; oil's flow into the food increases as consequence of an increase of air-oil interfacial tension, and a decrease of solid-oil interfacial tension and CA (Bouchon, 2009; Moreira et al., 1997; Ziaiifar et al., 2008).

Wettability is known to have an effect on heat and mass transfer processes, especially those in which the solid phase is porous and there are multiple fluid phases interacting (Udell, 1985). Brannan et al. (2014) defined wettability "as the affinity of a fluid for a solid", and highlighted its dependency on CA and interfacial tension. The wettability of a liquid on a solid surface can easily be determined by measuring its CA (Gomes Da Silva & Singh, 1995). As shown in Fig. 1, the CA has its vertex at the point where the immiscible phases meet, and each side is formed by the contact line between the solid–liquid and the liquid–gas interfaces (Bruus, 2007). If the CA is closer to 0° the liquid has a high wettability which means it can form a film on the solid's surface. On the other hand, if the value is higher than 90° the liquid forms droplets on top of the solid's surface due to its low wettability (Brannan et al., 2014; Rossi et al., 2009).

One of the first approaches to define the relationship between surface tension and CA at the equilibrium point was presented by Young at the beginning of the nineteenth century:

$$\gamma_{LG} \cos \theta_e = \gamma_{SG} - \gamma_{SL} \quad (1)$$

where $\gamma_{SG}$ is the solid–gas surface tension, $\gamma_{SL}$ is the solid–liquid interfacial tension, $\gamma_{LG}$ is the liquid–gas interfacial tension, and $\theta_e$ is the contact angle (Chaudhuri & Paria, 2009). From the four parameters in Young's equation only $\gamma_{LG}$ and $\theta_e$ are relatively easy to measure, and may be used to estimate solid surface tensions. However, it is necessary take into consideration the assumptions implicit in this equation which include: using a pure liquid and smooth homogeneous solid surface, $\gamma_{LG}>\gamma_{SG}$, and all interfacial tensions should remain constant while the measurements are performed (equilibrium state) (Kwok & Neumann, 2000; Volpe, Maniglio, Morra, & Siboni, 2002).

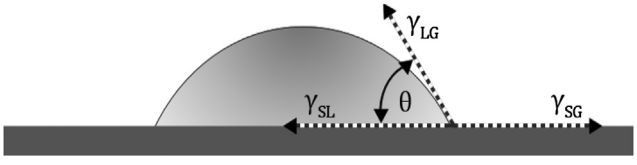


**Fig. 1.** Representation of the contact angle (θ) between solid–liquid ($\gamma_{SG}$) and liquid–gas ( $\gamma_{SL}$) interfaces.

In recent years, an increasing number of studies associating frequent consumption of deep-fried products (with high fat content) with the risk of developing illnesses such as: obesity, heart diseases, cancer and type 2 diabetes have been published (Cahill et al., 2014; Sayon-Orea et al., 2014; Stott-Miller, Neuhouser, & Stanford, 2013). Concurrently, consumer trends towards consumption of low-fat products have increased, and with them the interest of the food industry on lowering the oil uptake of deep-fried food to the minimum without affecting the quality of the product (Bouchon & Pyle, 2004). Thus, characterization of the wettability and surface properties is vital for better understanding solid–liquid interactions, as it opens the possibility for practical applications in the food industry such as surface modification to change the compatibility between phases (Adamson, 1990; Karbowiak, Debeaufort, & Voilley, 2006).

In order to better understand the effect of oil wettability in the absorption of oil into deep-fat fried foods, and develop frying processes that lead to lower oil uptake, it is necessary to understand how oil surface properties change during this process. Therefore, the aims of this work were to determine the effect of temperature, oil type, and surrounding media on the CA values of Canola and olive oils on PTFE, to evaluate predicted CA values for Canola and olive oils obtained from two mathematical models, and to determine the relationship between CA and liquid–gas interfacial tension values of Canola and olive oils measured at same conditions of temperature and surrounding media.

## 2. Materials and methods

### 2.1. Materials

Canola oil (ConAgra; Omaha NE, USA) and extra virgin olive oil (American Rice Inc.; Houston, TX, USA) were purchased from a local market. Polytetrafluoroethylene (PTFE or Teflon™) sheets AMS 3651 (152.4 × 152.4 × 1.5 mm) were bought from an online store (Amazon.com, Inc.).

### 2.2. Contact angle measurements

The equilibrium CA between each oil and PTFE film piece (26 × 7 mm) was measured by sessile drop method using a contact angle goniometer equipped with DROPimage software (Model 100 CA, P/N 190-F2; ramé-hart instrument co.; Succasunna NJ, USA). Drops were formed using a micro-syringe with 22 gauge stainless steel needles (P/N 100-10-20 and P/N 100-10-12-22 respectively; ramé-hart instrument co.; Succasunna NJ, USA). All measurements were performed inside an environmental chamber equipped with a temperature control system (P/N 100-07 and P/N 100-50 respectively; ramé-hart instrument co.; Succasunna NJ, USA), and using air or steam as the surrounding media. To avoid contamination, all surfaces were cleaned with acetone before and after each experiment, and allowed to dry for 1 min before starting a new measurement.

Prior to each set of experiments the goniometer was calibrated using a precision calibration device (P/N 100-27-31; ramé-hart instrument co.; Succasunna NJ, USA). CAs for Canola and olive oils were determined as baseline at room temperature (23 ± 1 °C) using air as the surrounding media, and at 110 °C using steam. Then temperature was increased and measurements were performed every 20 °C, starting at 40 °C for air and at 120 °C for steam, until the smoke temperature of each oil (180 °C for olive oil and 200 °C for Canola oil). A minimum of four measurements were performed at each temperature; however, additional measurements were

taken when variability was observed between the first two values obtained. Before performing a measurement, the system was allowed to equilibrate 1 min, and steady state was assumed if during that time no CA changes were observed. To prevent degradation of the oils by temperature, the total time for each measurement did not exceed 2–3 min.

In addition to the temperature controller of the environmental chamber, temperature was monitored using a digital handheld thermometer (Model HH21; OMEGA Engineering Inc.; Stamford CT, USA) and a pair of thermocouples. The first thermocouple was placed at the vicinity of the needle where the drop was generated. The second one was placed in between two PTFE sheets at the bottom of the environmental chamber, exactly underneath the point where the drop was deposited for the CA measurement.

### 2.3. Steam generation and delivery

Steam was generated by boiling distilled water in an Erlenmeyer flask on a hotplate stirrer. The flask was connected to a high temperature resistant pipe, which in turn was attached to a port of the environmental chamber (inlet port) (Fig. 2). The transfer pipe was covered by high temperature heating tape (O.E.M. Heaters; Saint Paul MN, USA) equipped with a temperature controller (OMEGA Engineering Inc.; Stamford CT, USA) to ensure the temperature of the steam was constant. In order to prevent heat loss and condensation, all the pipes and connections were covered with thermal insulation (Heatshield Products; Valley Center CA, USA) and aluminum foil. A Teflon lid was designed to stop steam from escaping through the top of the environment chamber; two holes were drilled into the lid one for the needle, and the other one to place a thermocouple. This ensured that steam only exited through a second port of the environmental chamber (outlet port) connected to a piece of tubing; condensation from this tube was collected in a beaker and monitored during each the experiment to verify that the steam was constantly flowing through the chamber. When air was used as surrounded media, both inlet and outlet ports of the environmental chamber remained closed.

### 2.4. Mathematical modeling of contact angle

CAs were predicted by the Girifalco-Good-Fowkes-Young (GGFY) equation (Eq. (2)) (Good & Girifalco, 1960), and GGFY equation combined with the Eötvös equation (Eq. (3)) that predicts the CA as a direct function of temperature (Eq. (4)).

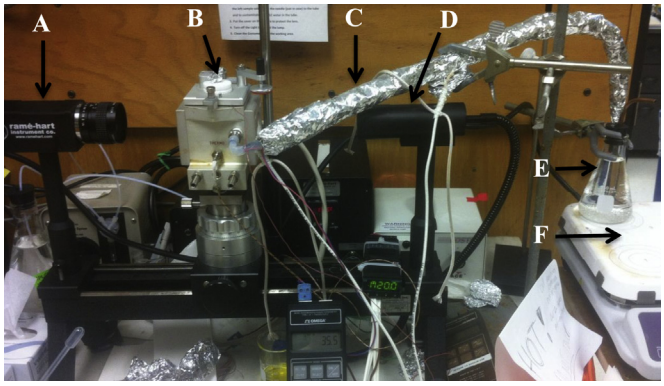


**Fig. 2.** Steam generation-delivery system, and goniometer parts: A) high resolution camera, B) environmental chamber, C) transfer pipe, D) light source, E) Erlenmeyer flask with distilled water, F) hotplate stirrer.

$$\cos\theta = -1 + 2\sqrt{\gamma_{SG}/\gamma_{LG}} \tag{2}$$

where $\gamma_{SG}$ is the solid–gas surface tension, $\gamma_{LG}$ is the liquid–gas interfacial tension, and $\theta$ is the contact angle.

$$\gamma_{LG}(M/\rho)^{\frac{2}{3}} = K_E(T_c - T) \tag{3}$$

Where $\gamma_{LG}$ is the liquid–gas surface tension, $M$ is the liquid molar mass, $\rho$ is the liquid density, $K_E$ is the Eötvös constant, $T_C$ is the liquid critical temperature, and $T$ is the sample temperature.

$$\cos\theta = -1 + 2\sqrt{\frac{\gamma_{SG}(M/\rho)^{2/3}}{K_E(T_c - T)}} \tag{4}$$

The percentage errors ($E$%) were calculated (Eq. (5)):

$$E\% = \frac{abs\left(\theta_{experimental} - \theta_{predicted}\right)}{\theta_{experimental}} \times 100 \tag{5}$$

The $\gamma_{SG}$ of PTFE used was 18 mN/m as previously reported by Goss (2010). This value was assumed to not change with temperature. The $M$ and $T_C$ values for Canola oil were 881.83 g/mol and 545.91 °C respectively, while the corresponding values for olive oil were 874.46 g/mol and 543.62 °C. The $T_C$, as well as, $\rho$ and $\gamma_{LG}$ reported in Table 1 were obtained from O'Meara (2012). Palit (1956) mentioned the effect of the molecules' geometry on the $K_E$; molecules almost spherical have lower values (e.g. mercury, $K_E \approx 1$) while more geometrically complex molecules have higher values (e.g. tripalmitine, $K_E = 5.4$). Thus, to obtain more accurate predictions, $K_E$ was adjusted for each of the four systems (oil-surrounding media) from 2.12 to approximately 6.1 dyn cm/mol$^{2/3}$K using Excel Solver and the Method of Least Squares.

### 2.5. Zisman's plots

To establish the relationship between liquid–gas interfacial tension and CA values, Zisman's plots were used. The solid–gas interfacial tension was estimated in terms of the critical surface tension of wetting ($\gamma_C$) which corresponds to the value of surface tension when $cos\theta_e = 1$ (Palakattukunnel, Thomas, Sreekumar, & Bandyopadhyay, 2011).

### 2.6. Statistical analysis

Data were analyzed using SAS 9.1.3 (SAS Institute Inc.; Cary NC,

**Table 1**
Density and liquid–gas interfacial tension values of Canola oil and Olive oil at different temperatures.

| T (°C) | Density[a] (g/cm$^3$) | | $\gamma_{LG}$[a] (mN/m) | | | |
|---|---|---|---|---|---|---|
| | Canola oil | Olive oil | Canola oil | | Olive oil | |
| | | | Air | Steam | Air | Steam |
| 23 ± 1 | 0.913 | 0.903 | 32.41 | | 32.03 | |
| 40 | 0.902 | 0.897 | 31.29 | | 30.91 | |
| 60 | 0.890 | 0.886 | 29.67 | | 29.47 | |
| 80 | 0.878 | 0.874 | 28.17 | | 28.11 | |
| 100 | 0.867 | 0.862 | 26.71 | | 26.51 | |
| 110 | 0.861 | 0.855 | – | 26.00 | – | 25.68 |
| 120 | 0.854 | 0.850 | 25.33 | 25.21 | 25.13 | 25.07 |
| 140 | 0.842 | 0.837 | 23.96 | 23.95 | 23.68 | 23.66 |
| 160 | 0.829 | 0.825 | 22.66 | 22.54 | 22.49 | 22.76 |
| 180 | 0.817 | 0.813 | 21.22 | 21.60 | 21.14 | 21.45 |
| 200 | 0.807 | – | 20.08 | 20.33 | – | – |

[a] O'Meara (2012).

USA). General Linear Model (GLM) and Regression (REG) analysis were performed on measured values of all individual data groups (Canola-air, Canola-steam, olive-air, and olive-steam). GLM was also performed for paired data groups by oil type or type of surrounding media, and all data combined. Tukey's test ($\alpha = 0.05$) was used to determine differences among measured data groups, as well as predicted values.

## 3. Results and discussion

### 3.1. Effect of temperature, oil type and surrounding media on the contact angles of Canola and olive oils on PTFE

CAs of Canola and olive oils on polytetrafluoroethylene (PTFE) were determined by sessile drop with a goniometer using air or steam as surrounding media (Table 2). PTFE was selected as the solid surface due to its low surface energy with values being reported between 18.0 and 25.6 mN/m (Fowkes, 1964; Fox & Zisman, 1950; Hamilton, 1972; Kerbow & Aten, 2009; Reardon & Zisman, 1974). Regardless of the oil type or surrounding media used, a significant decrease ($P < 0.05$) of CA values was observed as the temperature increased (Fig. 3).

Statistical analysis by General Linear Model (GLM) of all the data showed a significant effect ($P < 0.05$) of temperature and oil type on CA values, while no significant effect ($P > 0.05$) was appreciated by the surrounding media. The latest may be a consequence of not using saturated vapor, but superheated vapor which behavior approximately follows the ideal gas equation: $pV = nR_uT$; where $p$ is pressure, $V$ is volume, $n$ is molar amount, $R_u$ universal gas constant, and $T$ is temperature) (Dammel, Ochterbeck, & Stephan, 2009). The same analysis was performed to data subgroups classified by oil type, and also by surrounding media; results from GLM showed only the oil type variable had a significant effect ($P < 0.05$) when steam was used as surrounding media.

According to the Tukey mean comparison performed, no significant differences ($P > 0.05$) were observed above 120 °C regardless of the surrounding media used; this opens the possibility of obtaining good estimates for CAs values of oil-steam-PTFE at higher temperatures by using oil-air-PTFE data. Regardless of the oil type or surrounding media used, no significant differences ($P > 0.05$) were observed between CA pair values between 80 and 120 °C. At temperatures above and below, variation between pair values was a consequence of the difference on the rate of decrease in CA as the temperature increased between the oils.

**Table 2**
Comparison of the average contact angle values between each oil type (Canola oil or olive oil) and surrounding media (air or steam) at a set temperature.

| T (°C) | $\theta_e$ (°) | |
|---|---|---|
| | Canola oil | Olive oil |
| Air | | |
| 23 ± 1 | 61.8 ± 1.2$^{b}$ | 65.4 ± 1.0$^{a}$ |
| 40 | 58.6 ± 0.8$^{d}$ | 61.3 ± 0.5$^{c}$ |
| 60 | 54.5 ± 0.9$^{f}$ | 56.2 ± 0.9$^{e}$ |
| 80 | 51.5 ± 0.8$^{g}$ | 51.5 ± 1.3$^{g}$ |
| 100 | 47.9 ± 0.3$^{h}$ | 46.7 ± 0.4$^{h}$ |
| 120 | 43.9 ± 0.8$^{j}$ | 43.1 ± 0.6$^{j,k}$ |
| 140 | 40.2 ± 1.0$^{m}$ | 38.4 ± 0.7$^{n}$ |
| 160 | 37.6 ± 0.8$^{\circ}$ | 34.3 ± 0.6$^{p}$ |
| 180 | 34.4 ± 0.5$^{q}$ | 30.3 ± 0.4$^{r}$ |
| 200 | 30.3 ± 0.7$^{s}$ | – |
| Steam | | |
| 110 | 45.8 ± 0.9$^{i}$ | 44.2 ± 0.8$^{i}$ |
| 120 | 43.8 ± 0.3$^{j,k}$ | 42.0 ± 0.5$^{k}$ |
| 140 | 40.7 ± 0.6$^{m}$ | 38.3 ± 0.5$^{n}$ |
| 160 | 37.1 ± 0.6$^{\circ}$ | 33.8 ± 0.5$^{p}$ |
| 180 | 34.4 ± 0.3$^{q}$ | 30.3 ± 0.5$^{r}$ |
| 200 | 30.6 ± 0.4$^{s}$ | – |

±: corresponds to the standard deviation, $n \geq 4$.
[a]: Tukey mean comparison (95% Confidence) no significant difference between values sharing same letter.

Several studies mention CA to be dependent on temperature, decreasing as temperature increases. Only few studies have performed experiments to corroborate it; some of those studies used water on smooth cooper (Pointer, Davies, Beaton, & Ross, 1967), liquid metal on a ceramic surface (Rhee, 1971), organic liquids on a silicone glass surface (Neumann, 1974), water on a polished aluminum surface (Bernardin, Mudawar, Walsh, & Franses, 1997), or water on copper and aluminum surfaces (Hidaka, Yamashita, & Takata, 2006). Until recently, CA values of vegetable oils unused and used reported in the literature have been mainly determined at room temperature [e.g. Pinthus and Saguy (1994), Gomes Da Silva and Singh (1995), Yaghmur, Aserin, Mizrahi, Nerd, and Garti (2001), Dana and Saguy (2006)], giving valuable information about the effect of temperature on oil degradation, but failing to address its effect on surface properties.

In the present study, measured CAs decreased between the initial and final temperature following a linear trend (Eq. (6)), regardless of the oil type or surrounding media used (Fig. 4)

$$\theta_e = A + BT \tag{6}$$

where $\theta_e$ is the contact angle, $A$ is a constant, $B$ is the slope, and $T$ is the temperature in °C. This is similar to the results presented by Ashokkumar, Adler-Nissen, and Møller (2012) for CA of extra virgin olive oil on PTFE measured over a temperature range of 25–200 °C; however, their $cos\theta$ values varied approximately between 0.38 and 0.55 while the values of this study ranged from 0.42 to 0.86. These differences can be partially attributed to differences between oils' composition.

Regression analysis performed to each of the four data groups sorted by oil type and surrounding media allowed values for $A$, $B$ and correlation coefficient ($r^2$) for each line equation (Eq. (6)) to be determined (Table 3). It can be observed, as mentioned before, that the rate of decrease in CA as the temperature increase given by the slope ($B$) was different between oils being slightly higher for olive oil than for Canola oil. According to the wetting theory previously discussed, olive oil has a slightly higher wettability of PTFE than Canola oil at temperatures higher than 100 °C.

### 3.2. Mathematical modeling of contact angle

Contact angle values were predicted for each combination of temperature, oil and surrounding media as before using Girifalco-Good-Fowkes-Young (GGFY) equation (Eq. (2)), and a modification of equation (2) with the Eötvös equation (Eq. (3)) to give the GGFY-E (Eq. (4)). As established before CA ($\theta$) is temperature dependent, therefore when predicting CA values using the GGFY model it is necessary to know the liquid–gas interfacial tension ($\gamma_{LG}$) at the temperature or temperatures at which the prediction is desired. On the other hand, the GGFY-E model predicts CA as a function of temperature; however it is necessary to know the critical temperature of the fluid, and its density at the temperature at which CA is predicted. In both cases, the predicted values obtained were $cos\theta$ which were further converted into CA. The GGFY equation has been commonly used to determine surface free energy based on the geometry of liquid droplets (Gomes Da Silva & Singh, 1995; Park, Lee, Kim, & Jo, 2011). However, if the surface tensions of the solid and the liquid are known, it is possible to use it to calculate the $cos\theta$. The Eötvös equation describes the temperature dependence of the surface tension of the liquid (Restolho, Mata, & Saramago, 2009), and when substituted in the GGFY

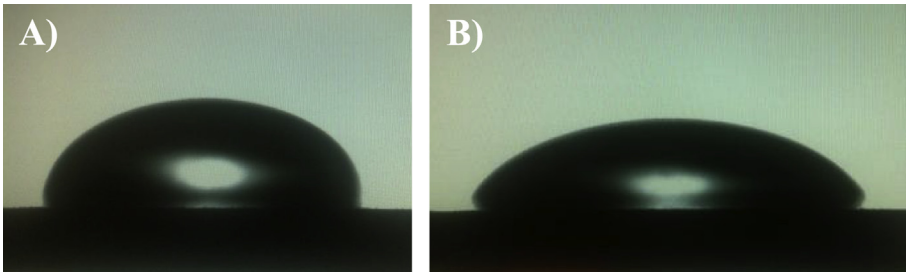


**Fig. 3.** Difference in contact angle (CA) of olive oil-air-PTFE by temperature. A) CA = 65.4° at room temperature (23 ± 1 °C), and B) CA = 30.3° at 180 °C.

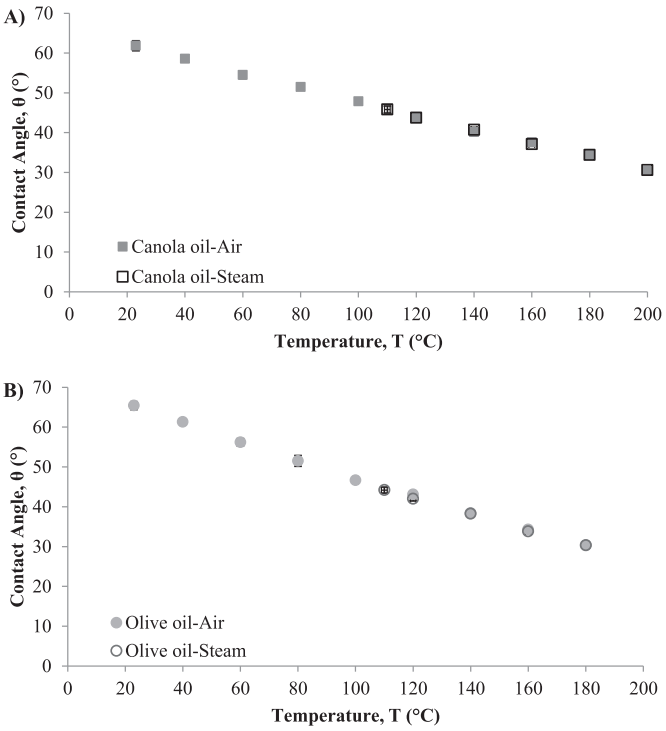


**Fig. 4.** Contact angles of A) Canola oil, and B) olive oil on polytetrafluoroethylene (PTFE) using air or steam as surrounding media.

**Table 3**
Intercept (A), slope (B) and correlation coefficient ($r^2$) values corresponding to the empirical equation for each data group to predict contact angle of Canola oil and olive oil on PTFE surrounded by air or steam.

| Oil type | Surrounding media | A | B | $r^2$ |
|---|---|---|---|---|
| Canola | Air | 65.397 | −0.175 | 0.992 |
| | Steam | 63.847 | −0.166 | 0.989 |
| Olive | Air | 69.876 | −0.223 | 0.994 |
| | Steam | 65.938 | −0.199 | 0.990 |

equation it is possible to determine the contact angle of a liquid–solid system taking into account the effect of temperature. Predicted CA values for Canola oil systems and their error percentage (*E*%) are reported in Table 4. Even though predicted values followed a similar trend as those obtained experimentally, only those predicted for Canola oil-air system at 40 and 160 °C were not significantly different ($P > 0.05$) from the experimental values. No significant difference ($P > 0.05$) was observed between the experimental value and the predicted value obtained with the GGFY-E equation at room temperature. Based on the error percentage, the majority of the values predicted for Canola oil-air and Canola oil-vapor systems by GGFY gave better estimates of the CAs than those predicted by GGFY-E, especially for the Canola oil-steam system. For both models, the highest *E*% values were obtained at the maximum temperature (200 °C), regardless of the surrounded media.

**Table 4**
Predicted contact angles for Canola oil on PTFE surrounded by air or steam by using Girifalco-Good-Fowkes-Young (GGFY) equation, and GGFY equation modified with the Eötvös equation (GGFY-E).

| T (°C) | $\theta_{e\ EXP}$ (°) | $\theta_{GGFY}$ (°) | $E\%_{GGFY}$ | $\theta_{GGFY-E}$ (°) | $E\%_{GGFY-E}$ |
|---|---|---|---|---|---|
| Air | | | | | |
| 23 ± 1 | $61.84^{a}$ | $60.63^{b}$ | 1.96 | $60.84^{a,b}$ | 1.62 |
| 40 | $58.56^{c}$ | $58.87^{c}$ | 0.54 | $58.77^{c}$ | 0.36 |
| 60 | $54.51^{e}$ | $56.10^{d}$ | 2.92 | $56.23^{d}$ | 3.16 |
| 80 | $51.50^{g}$ | $53.22^{f}$ | 3.34 | $53.39^{f}$ | 3.67 |
| 100 | $47.86^{i}$ | $50.07^{h}$ | 4.62 | $50.32^{h}$ | 5.13 |
| 120 | $43.85^{k}$ | $46.69^{j}$ | 6.47 | $46.75^{j}$ | 6.61 |
| 140 | $40.16^{m}$ | $42.82^{l}$ | 6.63 | $42.72^{l}$ | 6.39 |
| 160 | $37.57^{n}$ | $38.51^{n}$ | 2.51 | $38.01^{n}$ | 1.18 |
| 180 | 34.42° | $32.65^{p}$ | 5.15 | $32.32^{p}$ | 6.10 |
| 200 | $30.34^{q}$ | $26.67^{r}$ | 12.08 | $25.06^{s}$ | 17.39 |
| Steam | | | | | |
| 110 | $45.82^{b}$ | $48.39^{a}$ | 5.61 | $48.88^{a}$ | 6.68 |
| 120 | $43.77^{d}$ | $46.37^{c}$ | 5.94 | $47.05^{c}$ | 7.48 |
| 140 | $40.73^{f}$ | $42.79^{e}$ | 5.05 | $43.05^{e}$ | 5.70 |
| 160 | $37.12^{h}$ | $38.07^{g}$ | 2.57 | $38.38^{g}$ | 3.41 |
| 180 | $34.43^{j}$ | $34.34^{i}$ | 0.27 | $32.76^{i}$ | 4.84 |
| 200 | $30.59^{k}$ | $28.13^{l}$ | 8.06 | $25.63^{m}$ | 16.21 |

[a]: Values from the same row sharing the same letter are not significantly different ($P > 0.05$).

**Table 5**
Predicted contact angle values for olive oil on PTFE surrounded by air or steam by using Girifalco-Good-Fowkes-Young (GGFY) equation, and GGFY equation modified with the Eötvös equation (GGFY-E).

| T (°C) | $\theta_{e\ EXP}$ (°) | $\theta_{GGFY}$ (°) | $E\%_{GGFY}$ | $\theta_{GGFY-E}$ (°) | $E\%_{GGFY-E}$ |
|---|---|---|---|---|---|
| Air | | | | | |
| 23 ± 1 | $65.40^{a}$ | $60.05^{b}$ | 8.18 | $60.27^{b}$ | 7.84 |
| 40 | $61.32^{c}$ | $58.25^{d}$ | 5.00 | $58.38^{d}$ | 4.79 |
| 60 | $56.20^{e}$ | $55.73^{e}$ | 0.84 | $55.79^{e}$ | 0.74 |
| 80 | $51.52^{g}$ | $53.10^{f}$ | 3.07 | $52.94^{f}$ | 2.76 |
| 100 | $46.66^{i}$ | $49.61^{h}$ | 6.32 | $49.74^{h}$ | 6.60 |
| 120 | $43.10^{k}$ | $46.16^{j}$ | 7.10 | $46.17^{j}$ | 7.12 |
| 140 | $38.40^{m}$ | $41.95^{l}$ | 9.24 | $42.03^{l}$ | 9.45 |
| 160 | 34.31° | $37.88^{n}$ | 10.42 | $37.25^{n}$ | 8.58 |
| 180 | $30.35^{q}$ | $32.27^{p}$ | 6.36 | $31.31^{p,q}$ | 3.19 |
| Steam | | | | | |
| 110 | $44.17^{b}$ | $47.59^{a}$ | 7.74 | $48.30^{a}$ | 9.35 |
| 120 | $42.01^{d}$ | $46.00^{c}$ | 9.50 | $46.50^{c}$ | 10.69 |
| 140 | $38.27^{f}$ | $41.89^{e}$ | 9.47 | $42.40^{e}$ | 10.79 |
| 160 | $33.84^{i}$ | $38.87^{h}$ | 14.87 | $37.67^{g}$ | 11.32 |
| 180 | $30.32^{l}$ | $33.68^{k}$ | 11.11 | $31.81^{j}$ | 4.93 |

[a]: Values from the same row sharing the same letter are not significantly different ($P > 0.05$).

In the case of olive oil systems (Table 5), predicted CAs also followed a similar trend as the experimental values; however, *E*% values were larger. Values predicted for the olive oil-air system by both models at 60 °C were not significantly different ($P > 0.05$) from the experimental value. Similarly, this happened to the value predicted by the GGFY-E model at 180 °C. Contrary to results obtained for Canola oil-air system, the GGFY-E model gave the closest CA estimates for olive oil-air system, while the GGFY model predictions were closer to the experimental CA values for olive oil-steam system. Larger *E*% values were obtained when predicting the CAs of olive oil-steam system regardless of the model used.

As it can be observed in Fig. 5, predicted values obtained by both models fit closer with experimental CAs obtained for the Canola-air system than the olive oil-air system; this was also true for both oil-steam systems. CA values paired by temperature predicted by the GGFY and the GGFY-E equations were not significantly different ($P > 0.05$) from each other, with the exception of Canola oil systems at 200 °C, and olive oil-steam system at 160 and 180 °C.

### 3.3. Relationship between interfacial tension and contact angle

The Zisman approach was utilized to establish the relationship between interfacial tension and CA values of Canola oil and olive oil systems. This method allows an estimate of the surface tension of a solid phase (in this case PTFE) by measuring the CA of homologous liquids with progressively smaller surface tensions, and then plotting $\gamma_{LG}$ versus $cos\theta$ (Kabza, Gestwicki, & McGrath, 2000). In this study, variation of CA and liquid surface tension was caused by changing the temperature rather than using different liquids (Fig. 6). Zisman defined the critical surface tension of wetting ($\gamma_C$) as the value of surface tension of the liquid corresponding to $cos\theta_e = 1$; however the assumption that $\gamma_C$ gives a good estimate of the solid surface tension is limited to the liquids used to determine

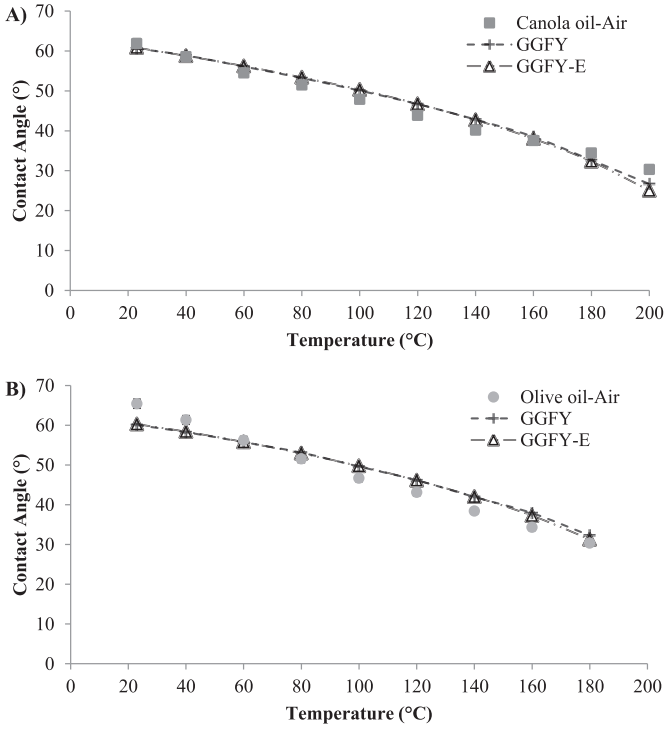


**Fig. 5.** Comparison between contact angle experimental values of A) Canola oil-air, and B) olive oil-air and their corresponding predicted values by Girifalco-Good-Fowkes-Young (GGFY) equation, and GGFY equation modified with the Eötvös equation (GGFY-E).

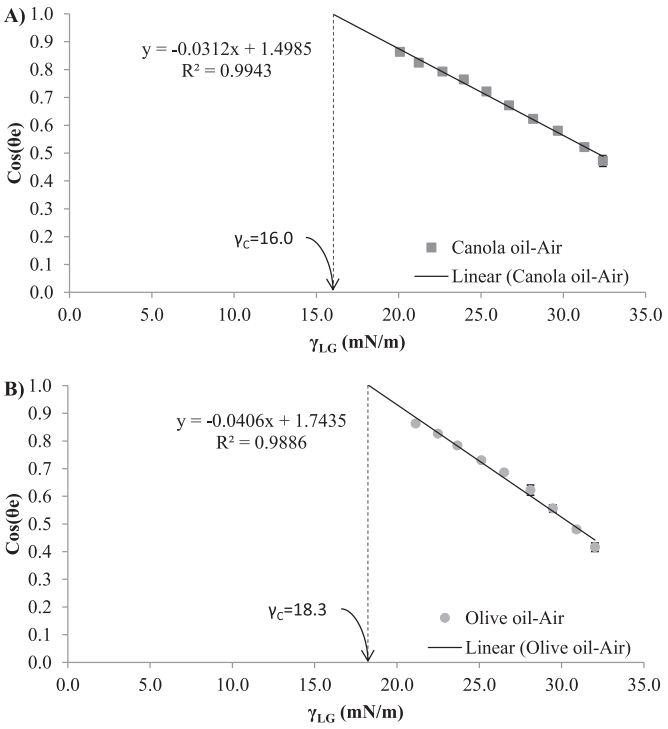


**Fig. 6.** Zisman plots for A) Canola oil-air and B) olive oil-air systems showing the critical surface tension.

it (Palakattukunnel et al., 2011).

The critical surface tension of PTFE using Canola oil and olive oil surrounded by air were calculated as 16.0 and 18.3 mN/m, respectively. Even though, the value obtained from the Canola oil-air system was smaller than the value reported in the literature (18 mN/m), it is important to considered that there is an implicit effect of the temperature in the experiment used here as only one liquid was used to calculate this value; meanwhile, reported values in the literature come from correlating interfacial tension and CAs obtained at one temperature from homologous liquids with different surface tensions.

## 4. Conclusions

Based on the results, an effect of temperature on CAs of Canola and olive oils on PTFE was corroborated; as temperature increased, the CAs decreased in all cases to a value close to 30°. There was a slight difference in how CAs of each type of oil decreased with increasing temperature; values corresponding to olive oil decreased at an approximate rate of 0.2°/°C for both air and steam conditions, while those of Canola oil decreased at 0.18 and 0.17°/°C respectively. No effect of the surrounding media was observed; thus, it is possible to use CA values of oil-air systems as estimates of oil-steam systems. Regardless of the mathematical models use to predict CA for Canola and olive oils on PTFE, the GGFY equation gave the closest estimates for both Canola oil systems, while the GGFY-E predicted better CAs for both olive oil systems. Slightly higher error percentage values were observed on predicted values for olive oil systems, especially on those predicted for olive oil-steam. By establishing the linear correlation between CA values and interfacial tension of Canola oil-air and olive oil-air systems, it was possible to estimate the solid surface tension of PTFE which allowed the verification of the data.

## Acknowledgement

We would like to thank the Center for Advanced Processing and Packaging Studies (CAPPS) for providing funding for this research project.

## References

Adamson, A. W. (1990). *Physical chemistry of surfaces* (5th ed.). New York: Wiley.

Ashokkumar, S., Adler-Nissen, J., & Møller, P. (2012). Factors affecting the wettability of different surface materials with vegetable oil at high temperatures and its relation to cleanability. *Applied Surface Science, 263*, 86–94. http://dx.doi.org/10.1016/j.apsusc.2012.09.002.

Bernardin, J. D., Mudawar, I., Walsh, C. B., & Franses, E. I. (1997). Contact angle temperature dependence for water droplets on practical aluminum surfaces. *International Journal of Heat and Mass Transfer, 40*(5), 1017–1033. http://dx.doi.org/10.1016/0017-9310(96)00184-6.

Blumenthal, M. M. (1991). A new look at the chemistry and physics of deep-fat frying. *Food technology, 45*(2), 68–71.

Bouchon, P. (2009). Understanding oil absorption during Deep-Fat frying. In L. T. Steve (Ed.), *Advances in food and nutrition research* (pp. 209–234). Academic Press.

Bouchon, P., & Pyle, D. L. (2004). Studying oil absorption in restructured potato chips. *Journal of Food Science, 69*(3), FEP115–FEP122. http://dx.doi.org/10.1111/j.1365-2621.2004.tb13363.x.

Brannan, R. G., Mah, E., Schott, M., Yuan, S., Casher, K. L., Myers, A., et al. (2014). Influence of ingredients that reduce oil absorption during immersion frying of battered and breaded foods. *European Journal of Lipid Science and Technology, 116*(3), 240–254. http://dx.doi.org/10.1002/ejlt.201200308.

Bruus, H. (2007). *Theoretical microfluidics*. Oxford: Oxford University Press.

Cahill, L. E., Pan, A., Chiuve, S. E., Sun, Q., Willett, W. C., Hu, F. B., et al. (2014). Fried-food consumption and risk of type 2 diabetes and coronary artery disease: a prospective study in 2 cohorts of US women and men. *The American Journal of Clinical Nutrition, 100*(2), 667–675. http://dx.doi.org/10.3945/ajcn.114.084129.

Chaudhuri, R. G., & Paria, S. (2009). Dynamic contact angles on PTFE surface by aqueous surfactant solution in the absence and presence of electrolytes. *Journal of Colloid and Interface Science, 337*(2), 555–562. http://dx.doi.org/10.1016/j.jcis.2009.05.033.

Dammel, F., Ochterbeck, J., & Stephan, P. (2009). Thermodynamics. In K.-H. Grote, & E. K. Antonsson (Eds.), *Springer handbook of mechanical engineering* (pp. 223–294). Springer Berlin Heidelberg.

Dana, D., & Saguy, I. S. (2006). Review: mechanism of oil uptake during deep-fat frying and the surfactant effect-theory and myth. *Advances in Colloid and Interface Science, 128–130*, 267–272. http://dx.doi.org/10.1016/j.cis.2006.11.013.

Erickson, M. D. (2007). Production and composition of frying fats. In M. D. Erickson (Ed.), *Deep frying – Chemistry, nutrition, and practical applications* (2nd ed., pp. 3–13). Urbana IL: AOCS Press.

Fowkes, F. M. (1964). Attractive forces at interfaces. *Industrial & Engineering Chemistry, 56*(12), 40–52. http://dx.doi.org/10.1021/ie50660a008.

Fox, H. W., & Zisman, W. A. (1950). The spreading of liquids on low energy surfaces. I. polytetrafluoroethylene. *Journal of Colloid Science, 5*(6), 514–531. http://dx.doi.org/10.1016/0095-8522(50)90044-4.

Gomes Da Silva, M., & Singh, R. P. (1995). Viscosity and surface tension of corn oil at frying temperatures. *Journal of Food Processing and Preservation, 19*(4), 259–270. http://dx.doi.org/10.1111/j.1745-4549.1995.tb00293.x.

Good, R. J., & Girifalco, L. A. (1960). A theory for estimation of surface and interfacial energies. III. Estimation of surface energies of solids from contact angle data. *The Journal of Physical Chemistry, 64*(5), 561–565. http://dx.doi.org/10.1021/j100834a012.

Gunstone, F. D. (2002). Food applications of lipids. In C. C. Akoh, & D. B. Min (Eds.), *Food lipids: Chemistry, nutrition, and biotechnology* (2nd ed.). New York, NY: Marcel Dekker, Inc.

Hamilton, W. C. (1972). A technique for the characterization of hydrophilic solid surfaces. *Journal of Colloid and Interface Science, 40*(2), 219–222. http://dx.doi.org/10.1016/0021-9797(72)90011-2.

Hidaka, S., Yamashita, A., & Takata, Y. (2006). Effect of contact angle on wetting limit temperature. *Heat Transfer—Asian Research, 35*(7), 513–526. http://dx.doi.org/10.1002/htj.20128.

Kabza, K. G., Gestwicki, J. E., & McGrath, J. L. (2000). Contact angle goniometry as a Tool for surface tension measurements of solids, using zisman plot method. A physical chemistry experiment. *Journal of Chemical Education, 77*(1), 63. http://dx.doi.org/10.1021/ed077p63.

Karbowiak, T., Debeaufort, F., & Voilley, A. (2006). Importance of surface tension characterization for food, pharmaceutical and packaging products: a review. *Critical Reviews in Food Science and Nutrition, 46*(5), 391–407. http://dx.doi.org/10.1080/10408390591000884.

Kerbow, D. L., & Aten, R. M. (2009). Poly(tetrafluoroethylene). In J. E. Mark (Ed.), *Polymer data handbook* (2nd ed., pp. 1060–1065). New York, NY: Oxford University Press.

Kochhar, S. P. (2001). The composition of frying oils. In J. B. Rossell (Ed.), *Frying – improving quality* (pp. 87–114). Boca Raton FL: Woodhead Publishing.

Kwok, D. Y., & Neumann, A. W. (2000). Contact angle interpretation in terms of solid surface tension. *Colloids and Surfaces A: Physicochemical and Engineering Aspects, 161*(1), 31–48. http://dx.doi.org/10.1016/S0927-7757(99)00323-4.

Mellema, M. (2003). Mechanism and reduction of fat uptake in deep-fat fried foods. *Trends in Food Science & Technology, 14*(9), 364–373. http://dx.doi.org/10.1016/S0924-2244(03)00050-5.

Moreira, R. G., Sun, X., & Chen, Y. (1997). Factors affecting oil uptake in tortilla chips in deep-fat frying. *Journal of Food Engineering, 31*(4), 485–498. http://dx.doi.org/10.1016/S0260-8774(96)00088-X.

Neumann, A. W. (1974). Contact angles and their temperature dependence: thermodynamic status, measurement, interpretation and application. *Advances in Colloid and Interface Science, 4*(2–3), 105–191. http://dx.doi.org/10.1016/0001-8686(74)85001-3.

O'Meara, M. (2012). *Determination of the interfacial tension between oil-steam and oil-air at elevated temperatures*. Master's thesis. North Carolina State University. Retrieved from: http://www.lib.ncsu.edu/resolver/1840.16/8150.

Palakattukunnel, S., Thomas, S., Sreekumar, P. A., & Bandyopadhyay, S. (2011). Poly(ethylene-co-vinyl acetate)/calcium phosphate nanocomposites: contact angle, diffusion and gas permeability studies. *Journal of Polymer Research, 18*(6), 1277–1285. http://dx.doi.org/10.1007/s10965-010-9530-1.

Palit, S. R. (1956). Thermodynamic interpretation of the eötvös constant. *Nature, 177*(4521). http://dx.doi.org/10.1038/1771180a0, 1180–1180.

Park, B. H., Lee, M.-H., Kim, S. B., & Jo, Y. M. (2011). Evaluation of the surface properties of PTFE foam coating filter media using XPS and contact angle measurements. *Applied Surface Science, 257*(8), 3709–3716. http://dx.doi.org/10.1016/j.apsusc.2010.11.116.

Pinthus, E. J., & Saguy, I. S. (1994). Initial interfacial tension and oil uptake by deep-fat fried foods. *Journal of Food Science, 59*(4), 804–807. http://dx.doi.org/10.1111/j.1365-2621.1994.tb08132.x.

Pointer, A. B., Davies, G. A., Beaton, W., & Ross, T. K. (1967). The measurement of contact angles under conditions of heat transfer when a liquid film breaks on a vertical surface. *International Journal of Heat and Mass Transfer, 10*(11), 1633–1636. http://dx.doi.org/10.1016/0017-9310(67)90017-8.

Reardon, J. P., & Zisman, W. A. (1974). Critical surface tensions of tetrafluoro-ethylene-perfluoro(propyl vinyl ether) copolymers. *Macromolecules, 7*(6), 920–923. http://dx.doi.org/10.1021/ma60042a042.

Restolho, J., Mata, J. L., & Saramago, B. (2009). On the interfacial behavior of ionic liquids: surface tensions and contact angles. *Journal of Colloid and Interface Science, 340*(1), 82–86. http://dx.doi.org/10.1016/j.jcis.2009.08.013.

Rhee, S. K. (1971). Wetting of ceramics by liquid metals. *Journal of the American Ceramic Society, 54*(7), 332–334. http://dx.doi.org/10.1111/j.1151-2916.1971.tb12307.x.

Rossi, M., Alamprese, C., Ratti, S., & Riva, M. (2009). Suitability of contact angle measurement as an index of overall oil degradation and oil uptake during frying. *Food Chemistry, 112*(2), 448–453. http://dx.doi.org/10.1016/j.foodchem.2008.05.101.

Saguy, I. S., & Dana, D. (2003). Integrated approach to deep fat frying: engineering, nutrition, health and consumer aspects. *Journal of Food Engineering, 56*(2–3), 143–152. http://dx.doi.org/10.1016/S0260-8774(02)00243-1.

Sayon-Orea, C., Bes-Rastrollo, M., Gea, A., Zazpe, I., Basterra-Gortari, F. J., & Martinez-Gonzalez, M. A. (2014). Reported fried food consumption and the incidence of hypertension in a mediterranean cohort: the SUN (Seguimiento Universidad de Navarra) project. *British Journal of Nutrition, 112*(06), 984–991. http://dx.doi.org/10.1017/S0007114514001755.

Stott-Miller, M., Neuhouser, M. L., & Stanford, J. L. (2013). Consumption of deep-fried foods and risk of prostate cancer. *The Prostate, 73*(9), 960–969. http://dx.doi.org/10.1002/pros.22643.

Udell, K. S. (1985). Heat transfer in porous media considering phase change and capillarity—the heat pipe effect. *International Journal of Heat and Mass Transfer, 28*(2), 485–495. http://dx.doi.org/10.1016/0017-9310(85)90082-1.

USDA-FAS. (2014). *Oilseeds: World markets and trade*. Retrieved from http://apps.fas.usda.gov/psdonline/circulars/oilseeds.pdf.

Volpe, C. D., Maniglio, D., Morra, M., & Siboni, S. (2002). The determination of a 'stable-equilibrium' contact angle on heterogeneous and rough surfaces. *Colloids and Surfaces A: Physicochemical and Engineering Aspects, 206*(1–3), 47–67. http://dx.doi.org/10.1016/S0927-7757(02)00072-9.

Yaghmur, A., Aserin, A., Mizrahi, Y., Nerd, A., & Garti, N. (2001). Evaluation of argan oil for deep-fat frying. *LWT - Food Science and Technology, 34*(3), 124–130. http://dx.doi.org/10.1006/fstl.2000.0697.

Ziaiifar, A. M., Achir, N., Courtois, F., Trezzani, I., & Trystram, G. (2008). Review of mechanisms, conditions, and factors involved in the oil uptake phenomenon during the deep-fat frying process. *International Journal of Food Science & Technology, 43*(8), 1410–1423. http://dx.doi.org/10.1111/j.1365-2621.2007.01664.x.